Received: 18 June 2021 | Accepted: 20 August 2021

DOI: 10.1002/pamm.202100109

Flow and fiber orientation of fresh fiber reinforced concrete

Florian Gerland[1,*], **Thomas Schomberg**[1], **Detlef Kuhl**[2], and **Olaf Wünsch**[1]

[1] Department of Fluid Dynamics, University of Kassel
[2] Institute of Mechanics and Dynamics, University of Kassel

The orientation of the fibers in UHPC is decisive for the tensile strength and failure of the components. The mold filling strategy during casting of structural components dictates the flow routing and thus the fiber orientation. In addition, the orientation of the fibers also affects the flow behavior of the suspension. In measurements of rheological properties in concrete rheometers, strongly scattering measurements often occur. In this paper, a novel fiber orientation model for viscoplastic fluids is investigated in Couette flow. The effect of the fibers on the flow condition and the measurable torque is described. The results of the numerical investigation give indications for increasing the reproducibility of rheological measurements on fresh fiber concrete.

1 Introduction

Due to their design, conventional concrete rheometers do not allow an analytical description of the flow inside. In a previous study, the flow state was therefore investigated numerically on the basis of the Bingham material [1]. This is even applicable for devices of arbitrary dimensions after some easy calibration experiments [2]. However, in fiber-reinforced concrete, the orientation of the fibers causes anisotropic flow behavior. Various experimental studies on the flow characteristics of fresh concrete containing fibers show strong variation even in the measured raw data. Often, the handling of pre-shearing is controversially discussed and referred as the cause for the different measurement results [3]. In this article, the influence of the orientation process on the measurable torque is investigated numerically. The applied orientation-dependent constitutive law, analytically derived on the basis of the slender-body theory, can be found in [4].

2 Numerical setup

The Couette flow of the fiber suspension based on a Bingham plastic matrix ($\tau_y = 5\,\mathrm{Pa}$, $\mu = 100\,\mathrm{Pa\,s}$) with $\Phi = 1\,\mathrm{vol}-\%$ fibers of aspect ratio $r = 60.6$ will be studied. The dimensionless cell radius was estimated to be $h/R = 18$. The fluid is located in the gap between two concentric cylinders, where the outer cylinder ($D_o = 0.24\,\mathrm{m}$) is driven at the rotational velocity $\Omega_o = 0.01\,\mathrm{rad/s}$, whilst the inner cylinder ($D_i = 0.15\,\mathrm{m}$) remains at rest (see fig. 1). The steady state analytical solution for a pure Bingham plastic under those conditions is applied for reference (dashed lines in fig. 4). Although a two-dimensional flow is studied, the fiber orientation should not be constrained in the third spatial direction (direction of rotation axis). The numerical experiment starts at time $t = 0\,\mathrm{s}$ from rest with an isotropic fiber orientation.

The flow is transient and incompressible and obeys mass and momentum balance given in eq. (1). The extra stresses consist of a matrix component $\mathbf{T}^\mathrm{m}$ (Bingham plastic) and a fiber component $\mathbf{T}^\mathrm{f}$ (eq. (2)) described by the Férec model.

$$\nabla\cdot\boldsymbol{v} = 0; \qquad \rho\left(\frac{\partial\boldsymbol{v}}{\partial t} + \nabla\boldsymbol{v}\cdot\boldsymbol{v}\right) = -\nabla p + \nabla\cdot\left(\mathbf{T}^\mathrm{m} + \mathbf{T}^\mathrm{f}\right) \tag{1}$$

$$\mathbf{T}^\mathrm{f} = \mu\phi\frac{2r^2}{3\log\left(h/R\right)}\mathbf{D} : \mathbf{A}_4 + \tau_y\phi\frac{r\left(h/R-1\right)}{\log\left(h/R\right)}\mathbf{A} \tag{2}$$

$$\frac{\mathrm{D}\mathbf{A}}{\mathrm{D}t} - \mathbf{L}^\mathrm{T}\cdot\mathbf{A} - \mathbf{A}\cdot\mathbf{L} = \begin{cases} -2\mathbf{D} : \mathbf{A}_4 + \frac{\tau_y}{\mu}\left(\frac{h/R-1}{a_r}\right)\left(\mathbf{I}-\alpha\mathbf{A}\right) & \text{for } |\tau| < |\tau_y| \\ \mathbf{0} & \text{for } |\tau| < |\tau_y|\,. \end{cases} \tag{3}$$

Equation (3) is the evolution equation of the second order orientation tensor $\mathbf{A}$. The fourth order orientation tensor $\mathbf{A}_4$ has been approximated by the well established IBOF5-closure [5]. The matrix constitutive model $\mathbf{T}^\mathrm{m} = 2\eta(\dot\gamma)\mathbf{D}$ with the Bingham viscosity function $\eta_\mathrm{Bm}\left(\dot\gamma\right) = \tau_y/\dot\gamma + \mu$ is regularized by the Papanastasiou regularization [6] to circumvent singularity for vanishing shear rate. No-slip conditions apply to the cylinder walls while symmetry is taken into account in the direction of axis of rotation. The system is discretized by a structured grid with 40 cells in radial, 120 cells in circumferential and 6 cells in symmetry direction. The numerical solution with the finite volume method was obtained using OpenFOAM v1912 with a second order spatial discretization and a first order implicit time discretization.

* Corresponding author: e-mail fluiddynamics@uni-kassel.de, phone +49 561 804 2719, fax +49 561 804 2720

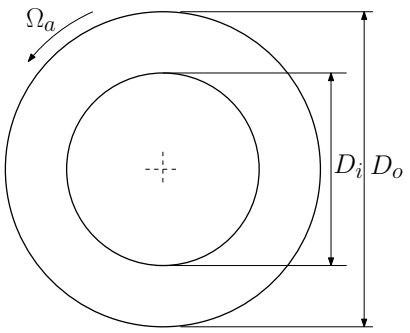

Fig. 1: Couette cell geometry.

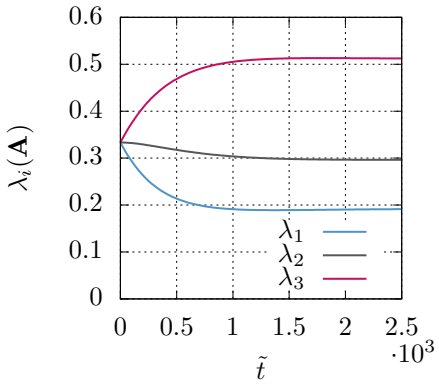

Fig. 2: Eigenvalues $\lambda_i(\mathbf{A})$) at ($\tilde{r} = 0$) over time.

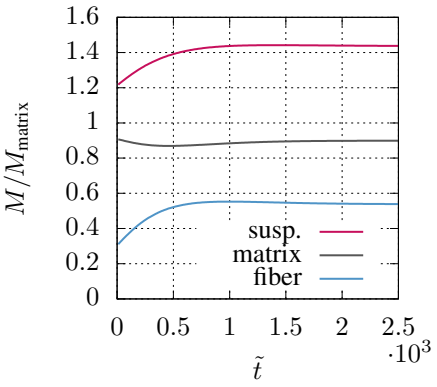

Fig. 3: Torque contributions of fibers and matrix. Rel. to steady state of matrix flow.

3 Results and Conclusion

The investigation has revealed that the time scale on which the fluid flow responds to the changed boundary conditions is several orders of magnitude higher than the orientation process of the fibers. After $\tilde{t} = \mu t / \left[\rho\,(R_a - R_i)^2\right] = 0.64$ the flow is pseudo-steady. At that point in time, almost no orientation has taken place (cp. fig. 2). Not before $\tilde{t} > 1000$, the flow is steady with no further alignment of the fibers. This can be seen as well in the torque shown in fig. 3. It increases by more than $40\,\%$ related to the pure matrix under the same conditions. Figure 4 shows the dimensionless rotational velocity $\tilde{\omega} = \omega/\Omega_o$ over the gap coordinate $\tilde{r} = (r - R_i)/(R_a - R_i)$. The additional fiber stress components have a significant effect on the flow field in the Couette flow. Under the same boundary conditions, the investigated suspension exceeds the yield point over the entire gap width, although the matrix fluid (dashed, blue) alone is not sheared in the region of the outer cylinder. For this simple flow pattern, which is also adopted in some occasions for fiber-reinforced mortars and UHPC in concrete rheometers, the rotational velocity profile of the fiber suspension corresponds almost ideally to a pure Bingham material (dashed, orange). This Bingham substitute model does not show an increased yield point compared to the matrix fluid, but it does exhibit an increased plastic viscosity ($\mu_{\text{eff}} = 210\,\text{Pa s}$). As can be recognized in fig. 5, the strain rate significantly decreases towards the outer cylinder. Hence, the orientation ellipsoides show nearly no alignment at the outer cylinder and a maximum preferential orientation at the inner cylinder, which does not coincide with the velocity direction. The material parameters, geometry and boundary conditions selected in the study are comparable to those expected in fresh concrete tests in concrete rheometers of this design. The duration of the orientation process extends into the typical measurement intervals. With a correspondingly long pre-shear, the orientation process can be excluded from the actual measurement curves for such measurements. In the literature, not all measurement descriptions contain information about pre-shearing. Therefore, this effect can be assumed to be a possible cause for the strong scattering of experimental results.

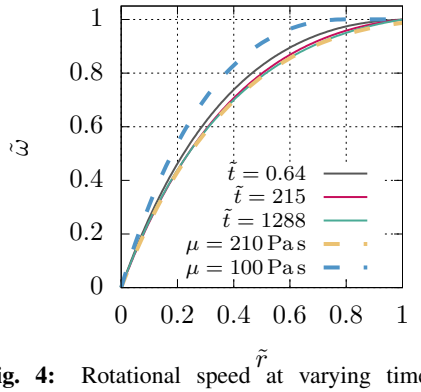

Fig. 4: Rotational speed at varying time. Dashed: steady state analytical Binham plast.

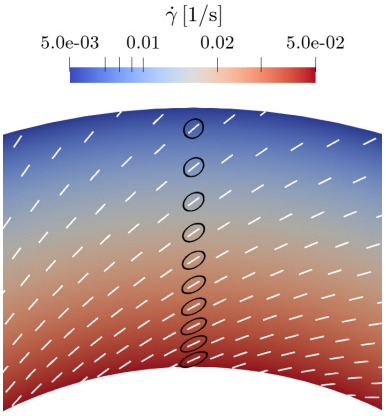

Fig. 5: Orientation and strainrate in steady state.

Acknowledgements Open access funding enabled and organized by Projekt DEAL.

References

[1] F. Gerland, A. Wetzel, T. Schomberg, O. Wünsch, and B. Middendorf, Appl. Rheol. **29**(1), 130–140 (2019).
[2] F. Gerland, T. Schomberg, A. Wetzel, B. Middendorf, and O. Wünsch, Proc. Appl. Math. Mech. **20**(1), e202000034 (2021).
[3] F. Gerland, M. Schleiting, T. Schomberg, O. Wünsch, A. Wetzel, and B. Middendorf, The effect of fiber geometry and concentration on the flow properties of UHPC, in: Rheology and Processing of Construction Materials, edited by V. Mechtcherine, K. Khayat, and E. SecrieruRILEM Bookseries (Springer International Publishing, 2019), pp. 482–490.

[4] J. Férec, E. Bertevas, B. C. Khoo, G. Ausias, and N. Phan-Thien, Physics of Fluids **29**(7), 073103 (2017).
[5] D. H. Chung and T. H. Kwon, Journal of Rheology **46**(1), 169–194 (2002).
[6] T. C. Papanastasiou, J. Rheol. **31**(5), 385–404 (1987).